A COMPARATIVE TEXTURE CLASSIFICATION STUDY BASED ON GENERALIZED COOCCURRENCE MATRICES

Larry S. Davis*
M. Clearman*
J. K. Aggarwal**

TR-110 August 1979

This paper will be presented at the IEEE Conference on Decision and Control, Miami FL, December 12-14, 1979.

* Computer Sciences Department
University of Texas
Austin Texas 78712

**Department of Electrical Engineering
University of Texas
Austin Texas 78712

This research was supported in part by the Air Force Office of Scientific Research under contract F49620-C-0043 and grant AFOSR 77-3190.

A COMPARATIVE TEXTURE CLASSIFICATION STUDY BASED ON GENERALIZED COOCCURRENCE MATRICES

Larry S. Davis,* M. Clearman,* and J. K. Aggarwal**

Abstract

A comparative study of generalized cooccurrence texture analysis tools is presented. A generalized cooccurrence matrix (GCM) reflects the shape, size and spatial arrangement of texture features. The particular texture features considered in this paper are: 1) pixel-intensity, for which generalized cooccurrence reduces to traditional cooccurrence; 2) edge-pixel; and 3) extended-edges. The best classification results, using pairs of descriptors computed from GCM's, were obtained using edge-pixel. This is consistent with the results reported in [4]. In addition, results are reported based on first-order statistics of edge-pixels and extended-edges.

1. Introduction

The ability to describe and discriminate between textures is crucial for the solution of many problems in image processing. A textured area in an image is characterized by a non-uniform, or varying, spatial distribution of intensity. The variation may be regular, such as the grating texture displayed in Figure 1a, or it may be more random, such as the swamp texture displayed in Figure 1b.

The intensity variation in an image texture ordinarily reflects some variation in the scene being imaged. For example, an image of mountainous terrain would appear textured. The specific appearance of that texture depends on the surface topography and albedo, the illumination of the surface, and the position and frequency response of the viewer. Or, as a second example, an X-ray of diseased tissue may appear textured due to the different absorption coefficients of healthy and diseased cells within the tissue.

There are, in general, two approaches to developing models for image texture. The first is to develop precise models for the scene being imaged, the illumination and the viewer. Image texture can, then, be theoretically related to the underlying physical scene variations (such as surface orientation). Such models are ordinarily very difficult to construct. Horn [1] has devoted a considerable amount of effort towards developing such models. The work by Barrow and Tenenbaum [2] on "intrinsic images" is also relevant.

The second approach treats the image texture directly, without specific regard to the physical basis of the image. Here, one hopes to develop computational tools which are generally useful for describing image texture. The tools may be designed with respect to some mathematical image model. For example, in [3], a variety of mosaic models were considered as mathematical models for image texture, and it was shown that such models could, in practice, be discriminated based on their variograms, which is the expected square difference in intensity between a pair of points as a function of distance between the points. Alternatively, the design of such tools may be motivated by less formal and more intuitive notions of what is "crucial" for describing texture. To a certain extent, one is almost always forced to rely on intuition and experience, since the mathematical image models almost never characterize the real textures at hand sufficiently well to be directly applied to their analysis.

This paper develops a tool for image texture analysis called a Generalized Cooccurrence Matrix, or GCM. GCM's were first introduced by Davis et al [4] as a general-purpose tool for image texture description. They are based on a model of image texture as a two-dimensional arrangement of texture elements, or primitives. So, for example, the texture in Figure 1a is a regular arrangement of diamonds. The texture in Figure 1b is not naturally described in terms of primitives and their arrangement. Therefore, the GCM model might not be appropriate for describing it.

GCM's do not describe textures by directly describing the shape and spatial arrangement of the texture elements (Maleson [5] describes such an approach). Rather, they describe the spatial arrangement of local image features, such as edges and lines. These local features are generally easier to compute than the texture elements themselves. Section 2 contains a more precise definition of GCM's. Such features are usually physically significant, i.e., they correspond to important physical discontinuities (reflectance, orientation, etc.) in the underlying scene. There is also psychophysical evidence that such local features play a prominent role in human texture perception [6].

Earlier image based approaches to texture description include those based on grey level cooccurrence matrices (Haralick et al [7]), grey level difference histograms (Rosenfeld et al [8]) and the power spectrum of the texture (Bajscy [9]).

Given an image, $I(x,y)$, $1 \le x,y \le n$ with $0 \le I(x,y) \le k$, k being the maximum grey level, the grey level cooccurrence matrix (GLCM) for that image at displacement $\Delta = (\Delta x, \Delta y)$, C_Δ, is defined by

$$C_\Delta(i_1,i_2) = \frac{\#\{((x,y),(x+\Delta x,y+\Delta y)):\ I(x,y)=i_1,\ I(x+\Delta x,y+\Delta y)=i_2\}}{\#\{((x,y),(x+\Delta x,y+\Delta y)):\ 1 \le x,y,x+\Delta x,y+\Delta y \le n\}}$$

where #S is the number of elements in set S. $C_\Delta(i_1,i_2)$ is an estimate of the probability that the grey level pair (i_1,i_2) will be found at a pair of image pixels separated by displacement Δ. The entries in C_Δ are thus called grey level cooccurrence probabilities. Various descriptors can be computed from C_Δ to describe the texture. For example, the "contrast" descriptor

$$\sum_{i=1}^{k} \sum_{j=1}^{k} (i-j)^2 C_\Delta(i,j)$$

can reflect the size of texture elements. For small Δ, low contrast ordinarily corresponds to texture elements which are wide in the direction of Δ. Haralick et al [7] discuss many other features. GCM's are a generalization of GLCM's which describe spatial distributions of local features rather than spatial distributions of intensity.

The grey level difference histograms, D_Δ, for displacement Δ, are defined by

$$D_\Delta(i) = \frac{\#\{((x,y),(x+\Delta x,y+\Delta y)):\ |I(x,y)-I(x+\Delta x,y+\Delta y)| = i\}}{\#\{((x,y),(x+\Delta x,y+\Delta y)):\ 1 \le x,y,x+\Delta x,y+\Delta y \le n\}}.$$

*Department of Computer Sciences
The University of Texas at Austin
Austin, Texas 78712
**Department of Electrical Engineering
The University of Texas at Austin
Austin, Texas 78712
This research was supported in part by the Air Force Office of Scientific Research under contract F49620-79-C-0043 and grant AFOSR 77-3190.

D_Δ contains less information than C_Δ because

$$D_\Delta(i) = \begin{cases} \sum_{j=0}^{k-i} C_\Delta(j,j+i) + \sum_{j=i}^{k} C_\Delta(j,j-i), & i \neq 0 \\ \sum_{j=0}^{k} C_\Delta(j,j), & i = 0 . \end{cases}$$

However, it is often true that descriptors computed from D_Δ describe textures as well as descriptors computed from C_Δ (see, e.g., the comparative study by Weszka et al [10]). In such a case D_Δ is preferable, since its storage requirements are lower than C.

Finally, the power spectrum of the texture can be used to compute texture descriptors. Let $P_I(\theta,r)$ be a polar representation of the power spectrum of I. Then texture descriptors reflecting texture element size can be computed from rings $R(r_1,r_2)$ in P_I where

$$R(r_1,r_2) = \int_{r_1}^{r_2} \int_{0}^{2\pi} P(\theta,r)d\theta dr.$$

Descriptors reflecting texture directionality can be computed from wedges, $W(\theta_1,\theta_2)$, in P_I where

$$W(\theta_1,\theta_2) = \int_{0}^{2\pi} \int_{\theta_1}^{\theta_2} P_I(\theta,r)d\theta dr.$$

Weszka et al [10] used, as descriptors, the intersection of rings and wedges, $RW(r_1,r_2,\theta_1,\theta_2)$ defined as

$$RW(r_1,r_2,\theta_1,\theta_2) = \int_{r_1}^{r_2} \int_{\theta_1}^{\theta_2} P_I(\theta,r)d\theta dr$$

but found such descriptors not as powerful as descriptors computed from D_Δ or C_Δ for texture classification. As Haralick [11] points out, this is not surprising, since for a texture which is Markov, the grey level cooccurrence probabilities can be used to compute the autocorrelation of the texture.

C_Δ, D_Δ and P_I are the most frequently used sources of texture descriptors, but many other sources have been proposed. Haralick's survey [11] contains an extensive review.

2. Generalized Cooccurrence Matrices

GCM's describe image textures by describing the spatial organization of image features. A particular GCM is defined by specifying

1) an image feature prototype, P,
2) a spatial predicate, S, and
3) a prototype attribute, A.

The prototype can be regarded as the structural definition of the image features of interest, or, more simply, as a list of prototype attributes. For example, the prototype edge-pixel can be defined as follows with three attributes

edge-pixel
location: (x,y), $1 \leq x,y \leq n$
orientation: θ, $0 \leq \theta \leq 2\pi$
contrast: C, $0 \leq C \leq k$

As a second example, consider the prototype extended edge

extended-edge
end1: (x_1,y_1), $1 \leq x_1,y_1 \leq n$
end2: (x_2,y_2), $1 \leq x_2,y_2 \leq n$
orientation: $\theta = \tan^{-1}\frac{y_1-y_2}{x_1-x_2}$, $0 \leq \theta \leq 2\pi$
length: $\ell = \sqrt{(x_1-x_2)^2+(y_2-y_1)^2}$, $0 \leq \ell \leq n\sqrt{2}$

Both of these prototypes will be used in the experiments described in Section 3.

A spatial predicate is a mapping from image feature pairs into {TRUE,FALSE}. For example, the spatial predicate S_k, defined over pairs of edge-pixels $((x_1,y_1),\theta_1,C_1),((x_2,y_2),\theta_2,C_2)$, is true if

$$\max\{|x_1-x_2|,|y_1-y_2|\} \leq k$$

Now, suppose we are given a set of image features $F = \{f_1,f_2,\ldots,f_m\}$, each of which is structured according to some given prototype definition. Let S be a given spatial predicate defined over that prototype and let A be the attribute of interest. We will let A_{f_i} refer to the value of the attribute for feature f_i. Then, the GCM, $G_{S,A}$ is defined by

$$G_{S,A}(v_1,v_2) = \frac{\#\{(f_i,f_j): A_{f_i}=v_1, A_{f_j}=v_2, S(f_i,f_j) = \text{TRUE}\}}{\#\{(f_i,f_j): S(f_i,f_j) = \text{TRUE}\}}$$

As an example, consider Figure 2. The prototype is edge-pixel. Figure 2a shows the spatial distribution of edge-pixels for some texture (a blank means that no edge-pixel feature was detected at that image point). An H stands for horizontal edge, V vertical, L left diagonal and R right diagonal. The attribute is orientation, θ, and the spatial predicate is S_1 which assigns true to all pairs of edge pixels within distance 1 of one another. Figure 2b shows the GCM, $G_{S_1,\theta}$.

Note that a grey level cooccurrence matrix, C_Δ, is a special case of a GCM with prototype

pixel-intensity
location: (x,y), $1 \leq x,y \leq n$
intensity: i, $0 \leq i \leq k$,

prototype attribute intensity, and a spatial predicate which assigns the value true to pairs of pixel-intensity features, $((x_1,y_1),i_1),((x_2,y_2),i_2)$, with either

$$x_1 = x_2+\Delta x, \quad y_1 = y_2+\Delta y \quad \text{or}$$
$$x_2 = x_1+\Delta x, \quad y_2 = y_1+\Delta y.$$

The experimental study described in Section 3 will compare the three prototypes: pixel-intensity, edge-pixel, and extended-edge. Before describing the details of that study, we will discuss the computation of the spatial predicates and descriptors which the study will use.

A. Pixel-intensity spatial predicates

Ordinarily, when computing a grey level cooccurrence matrix, rather than using a single displacement, Δ, one uses a set of displacements, $\mathcal{D} = \{\Delta_1,\Delta_2,\ldots,\Delta_m\}$. A cooccurrence matrix, $C_\mathcal{D}$, can then be defined by

$$C_\mathcal{D}(i,j) = \frac{1}{m}\sum_{h=1}^{m} C_{\Delta_h}(i,j)$$

We define the two sets

$\mathcal{D}_1 =$
$\{(0,1),(1,1),(1,0),(1,-1),(0,-1),(-1,-1),(-1,0),(-1,1)\}$
and $\mathcal{D}_2 = \{(0,2),(2,0),(0,-2),(-2,0)\}$

and then define the spatial predicates $S_{\mathcal{D}_h}$, $h = 1,2$ over pixel-intensity by

$S_{\mathcal{D}_h}(f_i,f_j)$ =

TRUE iff $x_1 = x_2+\Delta x$, $y_1 = y_2+\Delta y$, for $(\Delta x,\Delta y) \in \mathcal{D}_h$

Figures 3a and 3b illustrate the spatial predicates $S_{\mathcal{D}_1}$ and $S_{\mathcal{D}_2}$.

B. Edge-pixel spatial predicates

Three spatial predicates will be used to compute GCM's for edge pixels. The first is S_k (defined previously) which is true if the distance between two edge-pixels is less than or equal to k.

The second spatial predicate examines a cone-shaped region of a fixed size along the orientation of an edge-pixel. Figure 4a illustrates this predicate, called S_{α_k}. The last spatial predicate examines a cone-shaped neighborhood of a fixed size which is orthogonal to the orientation of an edge-pixel. This predicate, $S_{\mathcal{O}_k}$, is illustrated in Figure 4b. For a feature pair f_i and f_j, both S_{α_k} and $S_{\mathcal{O}_k}$ evaluate to true if f_j lies in one of the appropriately oriented cones centered at f_i.

Intuitively, S_{α_k} and $S_{\mathcal{O}_k}$ should be useful for determining the elongatedness and width of the texture elements. For elongated texture elements, $G_{S_{\alpha_k},\theta}$ would have high values along the main diagonal since edges of elongated shapes tend to "line up". Similarly, for narrow texture elements, $G_{S_{\mathcal{O}_k},\theta}$ should have high values along the main diagonal.

C. Extended-edge spatial predicates

The extended-edge spatial predicates are similar to the edge-pixel spatial predicates. Two such spatial predicates will be defined: one which looks along the direction of the extended-edge, and one which looks orthogonal to the direction of the extended-edge.

Figure 5a illustrates the spatial predicate, S_{a_k}. $S_{a_k}(f_i,f_j)$ is true if one end of the extended-edge f_j lies in one of the k×k neighborhoods centered about either end of f_i. In this case f_i and f_j meet within that neighborhood of size k.

The other spatial predicate, S_{N_k}, is defined similarly, except that the neighborhoods emanate from the center of f_i (see Figure 5b).

Note that although the spatial predicates associated with extended-edges are more complex than those associated with edge-pixels, the overall computational effort of computing GCM's for extended-edges is comparable to that for edge-pixels since, in general, there are far fewer extended-edges than edge-pixels.

D. Descriptors

GCM's can be directly used to represent a texture class. However, it is ordinarily sufficient, for the purposes of classification, to represent a texture class by a small set of texture descriptors computed from the GCM. These descriptors are similar to the ones described by Haralick et al [7] for grey level cooccurrence matrices. They include:

1) Contrast--For a grey level cooccurrence matrix, C_Δ, the contrast descriptor was defined ([7]) as

$$\sum_i \sum_j (i-j)^2 \, C_\Delta(i,j).$$

For a GCM, $G_{S,A}$, contrast is defined similarly as

$$\sum_i \sum_j d(i,j) \, G_{S,A}(i,j).$$

Here, $d(i,j)$ is a dissimilarity measure which depends on A. For example, when A is orientation, we take $d(i,j) = |\sin(i-j)|$. When A is length or intensity, then we use $d(i,j) = (i-j)^2$.

2) Uniformity--The uniformity descriptor is defined by

$$\sum_i \sum_j (G_{S,A}(i,j))^2.$$

Uniformity is lowest when all elements of G have equal value.

3) Entropy--The entropy descriptor is defined by

$$\sum_i \sum_j -G_{S,A}(i,j) \log(G_{S,A}(i,j)).$$

4) Correlation--The correlation descriptor is defined by

$$\sum_i \sum_j \frac{(ijG_{S,A}(i,j) - u_i^r u_j^c)}{\sigma_i^r \sigma_j^c},$$

where u_i^r is the mean of the i^{th} row, u_j^c is the mean of the j^{th} column, σ_i^r is the standard deviation of the i^{th} row and σ_j^c is the standard deviation of the j^{th} column.

In [4], Davis et al discuss, informally, the relationship between these descriptors and various aspects of texture, such as shape, size and placement of the texture elements. Section 3 presents an experimental study using these descriptors for GCM's based on pixel-intensity, edge-pixel and extended-edge prototype features. In addition, classification results based on first-order statistics of edge-pixel attributes and extended-edge attributes are included.

3. Experimental Study

An experiment was designed and performed to compare the descriptive power of image features such as pixel-intensity, edge-pixel and extended-edge. Eight classes of natural textures were used. They are shown in Figure 6 and include brick, striated concrete, grating, metal scrap, orchard, pebbles, shrubs and tree bark. These images were digitized using a flying spot scanner system to a resolution of 256×256 pixels, with each pixel intensity digitized to six bits. The first-order grey level distributions of all of the textures were then normalized to uniform distributions, so that differences in brightness could not be used to discriminate the textures. The grey scale normalization procedure is described in Rosenfeld and Kak [12]. Sixteen 64×64 samples were then extracted from each digitized image, and these formed the database for the classification experiment. Figure 7 contains one sample from each class.

The study used a leave-one-out classifier. In this method, all samples but one in the data set are used as the training set. The remaining sample is then classified using the statistics derived from the training set. The sample is classified using the following distance measure: Let $\bar{f}$ be the descriptor vector for an unknown example, and let $\bar{u}_c$ and $\bar{\sigma}_c$ be the mean and standard deviation vectors for class c. Then the distance from $\bar{f}$ to class c is

$$\sqrt{\frac{(\bar{f} - \bar{u}_c)^2}{\bar{\sigma}_c}}$$

The unknown is then assigned to the class for which this distance measure is minimal.

Before presenting the experimental results, the procedures for computing the image features edge-pixel and extended-edge will be described.

Edge-pixels are detected using an edge detection procedure based on an adaptation of the edge operator suggested by Kirsch [13]. The operator breaks the 5×5 neighborhood of a picture point, x, into the 9 regions shown in Figure 8. The contrast, C(x), of the edge operator at point x is then

$$\max_{i=0}^{7} \left| 5 * \sum_{j=0}^{2} r_{i+j} - 3 * \sum_{j=3}^{7} r_{i+j} \right|$$

with subscript addition computed modulo 8. Here, r_i is the average grey level in the i^{th} block. An orientation $\theta(x)$ is also associated with x, and is determined by the value of i which maximizes the above expression. For example, if i=0 maximizes the expression, then the orientation associated with x is horizontal. Let C(x) and $\theta(x)$ denote the contrast and orientation at point x. Then the following two step process detects edges based on C(x) and $\theta(x)$.

1) Threshold--Eliminate as edges all x with $C(x) < t$.
2) Peak selection--Consider the line segment of length 2d and orientation $\theta(x) + \pi/2$ passing through x. Eliminate x as an edge if there is an x' on this line with $C(x') > C(x)$.

Thresholding alone is not sufficient, since the edge operator gives high contrast not only to points at edges, but also to points near edges. Peak selection alone will not remove spurious, low-value peaks in the interiors of texture elements or in the background. Note that thresholding and peak selection commute, so that steps 1 and 2 could be reversed. Figure 9 shows the edge-pixels detected for the samples shown in Figure 7.

Extended-edges correspond to connected components of constant orientation edge-pixels. Each such connected component is represented by a line segment joining a suitably defined pair of extremal points. For example, for a component of horizontal edge-pixels, the line segment joins the left-most edge-pixel to the right-most edge-pixel. Figure 10 contains an example of extended-edges superimposed on top of an original grey scale texture.

The results of the experiment using descriptors from GCM's are summarized in Tables 1-2. For each prototype and spatial predicate, the best descriptor pair is listed along with the percentage classification. The results shown in Table 1 are consistent with those reported in [4]; the edge-pixel cooccurrence statistics give higher classification rates than the pixel-intensity cooccurrence statistics (61% vs. 52%). Of course, two features are not enough to provide satisfactory classification rates in either case. Adding more features leads to somewhat higher classification rates.

The poor results for extended-edge cooccurrence are at first surprising, since one would expect that the long edges would more naturally reflect the shapes of the texture elements. However, several factors contribute to their poor performance:

1) the number of extended-edges in any one texture sample is rather small, so that the GCM's are quite sparse. In such situations, the descriptors cannot be expected to be very reliable.
2) Extended-edges were computed using the simplest possible algorithm. The reason for choosing that algorithm was computational efficiency--the entire process of detecting edges and computing connected components of constant orientation can be accomplished in a single pass through the texture. A more complex procedure would have produced better extended-edges, but at the expense of higher computing costs.

We are currently pursuing several potential solutions to the second problem. One, for which preliminary results are not particularly encouraging, involves applying a "relaxation" procedure [14] to the output of the edge operator to enhance its results. This tends to be quite expensive and not to improve the orientation of the edges. A second, and more promising, approach is to develop optimal edge detection operators for cellular textures. This work is described in Davis and Mitiche [15].

Since others (Marr [16], Weszka et al [10]) have suggested that first-order statistics of edges should provide adequate texture descriptors, we performed the same classification experiment using pairs of first-order statistics of edge-pixels and extended-edges. For edge-pixels, the statistics considered were average orientation and standard deviation of orientation. For extended-edges, we considered average length and orientation, and standard deviation of length and orientation. The results were quite surprising, and are contained in Table 2. The sparsity of the extended-edge GCM helps to explain why first-order extended-edge statistics provide higher classification rates than GCM extended-edge descriptors. The results for pixel-edges are not as simple to explain. However, an important factor is that the GCM descriptors are invariant to rotations of the original textures. For example, in the contrast descriptor, the dissimilarity measure is based on the sine of the difference between two angles; that difference is invariant to the addition of a constant to each angle, which is the result of rotation. The first-order statistics, on the other hand, are not all rotation invariant. Average orientation was one of the best first-order edge-pixel statistics, and this statistic is obviously not invariant to rotations of the textures. One can see from the scatter plot in Figure 11 that if the gratings, G, had been rotated by 45°, they would have penetrated other clusters, and the classification accuracy would have been lowered.

4. Summary

In [4], GCM's were introduced as a new tool for image texture analysis, and the results of a small experimental study were reported comparing descriptors obtained from pixel-edge and pixel-intensity based GCM's. In this paper, we have also considered the prototype extended-edge, and the experimental study covered a much larger database and included a comparison of GCM descriptors with first-order statistics of pixel-edges and extended-edges. The results reported here are consistent with those reported in [4]; the edge based GCM's provided higher classification rates than the intensity based GCM's, which correspond to the conventional cooccurrence matrices. The higher classification rates obtained using first-order statistics should be interpreted cautiously, since, as discussed, the first-order statistics chosen were not all rotation invariant. For the database which we considered, where all samples of a texture were drawn from a single, larger frame in which the texture was "stationary", the rotational variance of some of the first-order statistics enhanced their classification power. In other situations this might not be true.

References

1. B.K.P. Horn, "Understanding Image Intensities," *Artificial Intelligence, 8,* pp. 201-231.
2. H. Barrow and J. M. Tenenbaum, "Recovering Intrinsic Scene Characteristics from Images,"

Computer Vision Systems, ed. A. Hanson and E. Riseman, Academic Press, NY, 1978.
3. B. Schachter, A. Rosenfeld and L. Davis, "Random Mosaic Models for Texture," *IEEET-Systems, Man and Cybernetics, 9*, pp. 694-702.
4. L. Davis, S. Johns and J. K. Aggarwal, "Texture Analysis Using Generalized Cooccurrence Matrices," *IEEET-Pattern Analysis and Machine Intelligence, 1*, pp. 251-258.
5. J. Maleson, C. Brown and J. Feldman, "Understanding Natural Textures," in *Proc. DARPA Image Understanding Workshop*, Palo Alto, CA, 1977, pp. 19-27.
6. B. Julesz, "Differences between Attentive (Figure) and Preattentive (Ground) Perception," in *Proc. Image Modelling Workshop*, ed. A. Rosenfeld, to appear.
7. R. Haralick, B. Shanmugam and I. Dinstein, "Texture Features for Image Classification," *IEEET-Systems, Man and Cybernetics, 3*, pp. 610-622.
8. A. Rosenfeld and E. Troy, "Visual Texture Analysis," *Conf. Record for Symposium on Feature Extraction and Selection in Pattern Recognition*, IEEE Press, 1970, pp. 115-124.
9. R. Bajscy and L. Lieberman, "Texture Gradient as a Depth Cue," *Computer Graphics and Image Processing, 5*, 1976, pp. 52-67.
10. J. Weszka, C. Dyer and A. Rosenfeld, "A Comparative Study of Texture Measures for Terrain Classification," *IEEET-Systems, Man and Cybernetics, 4*, 1976, pp. 269-285.
11. R. Haralick, "Statistical and Structural Approaches to Texture," *Proc. IEEE, 67*, 1979, pp. 786-805.
12. A. Rosenfeld and A. Kak, *Digital Picture Processing*, Academic Press, NY, 1976.
13. R. Kirsch, "Computer Identification of the Constituent Structure of Biological Images," *Computers and Biomedical Research, 4*, 1971, pp. 315-328.
14. A. Rosenfeld, R. Hummel and S. Zucker, "Scene Labeling Using Relaxation Operations," *IEEET-Systems, Man and Cybernetics, 6*, 1976, pp. 420-433.
15. L. Davis and A. Mitiche, "Edge Detection in Textures," in *Proc. Image Modelling Workshop*, ed. A. Rosenfeld, to appear.
16. D. Marr, "Early Processing of Visual Information," *Phil. Trans. Royal Society, B, 275*, 1976, pp. 483-524.

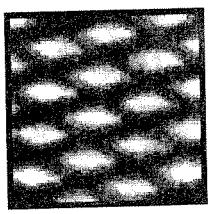

a) grating

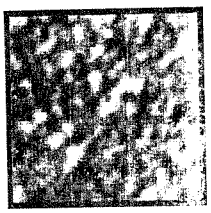

b) swamp

Figure 1. A regular and a random texture.

						H	H
	H	H	H		R		
L				R			
V				V			
V				V			
	H	H	H		L	H	H
L			V				V
V			V				V

a) edge-pixels

	H	V	L	R
H	12	6	3	2
V	6	8	3	1
L	3	3	0	0
R	2	1	0	2

b) $G_{S_1,\theta}$

Figure 2. A simple example of a GCM.

p_2	p_3	p_4
p_1	x	p_5
p_8	p_7	p_6

a) $S_{\mathcal{D}_1}(x,p_i)$ is TRUE for i=1,...,8

		p_2		
p_1		x		p_3
		p_4		

b) $S_{\mathcal{D}_2}(x,p_i)$ is TRUE for i=1,...,4

Figure 3. Pixel intensity spatial predicates.

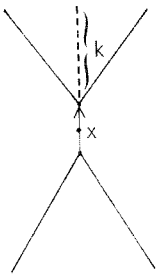

a) $S_{a_k}(x,y)$ is TRUE if y lies in one of the cones.

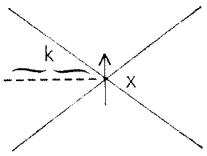

b) $S_{\mathcal{O}_k}(x,y)$ is TRUE if y lies in one of the cones.

Figure 4. Spatial predicates for edge-pixels.

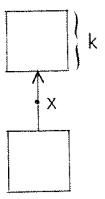

a) $S_{a_k}(x,y)$ is TRUE if one end of extended-edge y lies in either of the boxes surrounding the ends of x.

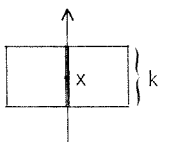

b) $S_{N_k}(x,y)$ is TRUE if one end of y lies in either of the boxes emanating from the center of x.

Figure 5. Spatial predicates for extended-edges.

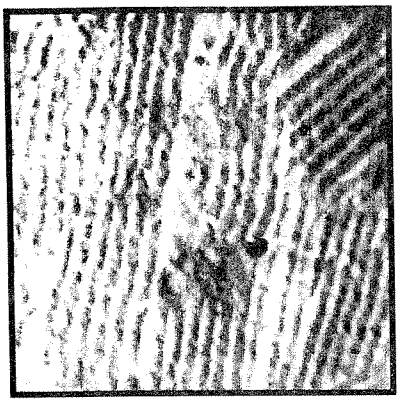

a) striated concrete (E)

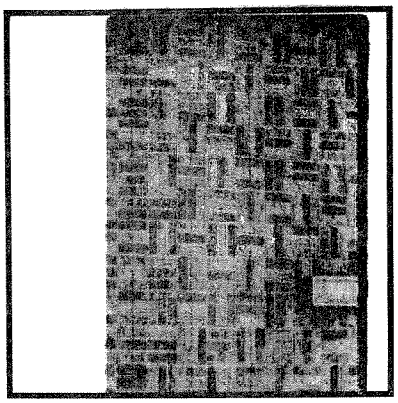

e) brick (B)

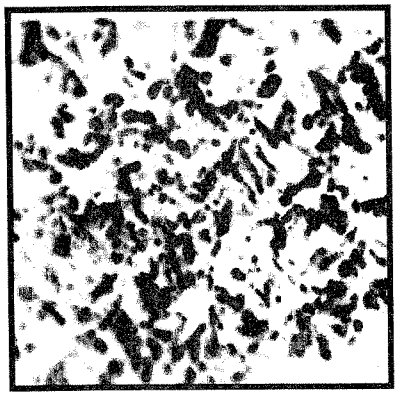

b) shrub (S)

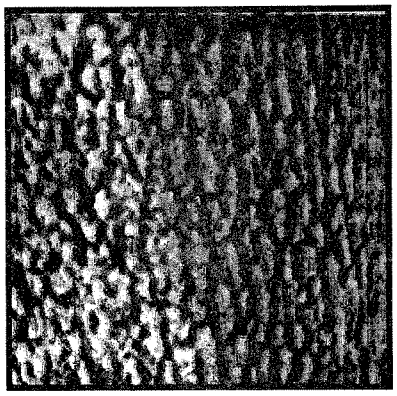

f) tree bark (T)

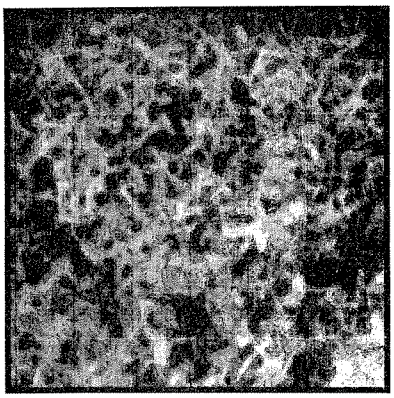

c) metal (M)

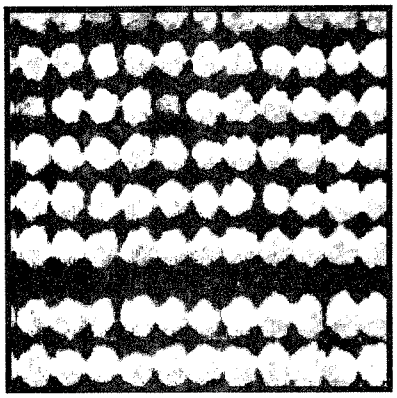

g) orchard (O)

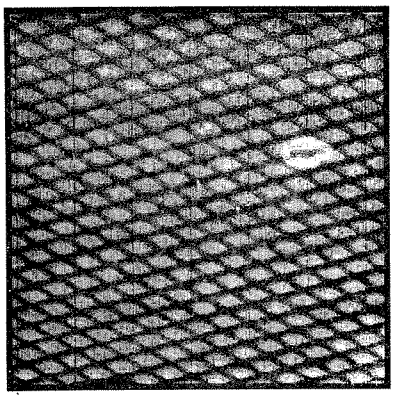

d) grating (G)

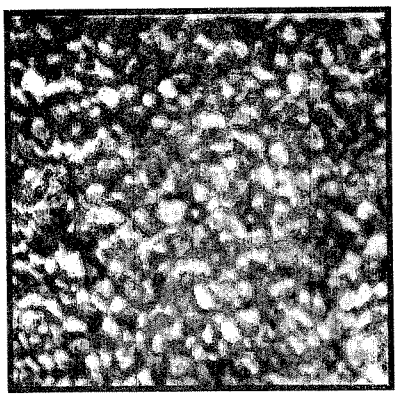

h) pebbles (P)

Figure 6. Texture classes -- single letter codes for scatter plots in parentheses.

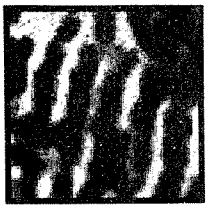

7a

(E)

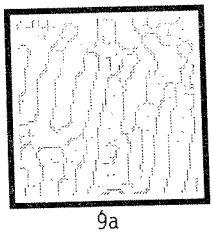

9a

7b

(S)

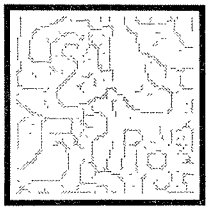

9b

7c

(M)

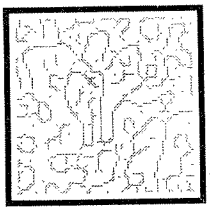

9c

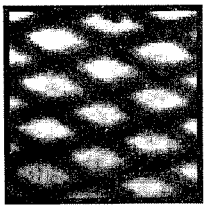

7d

(G)

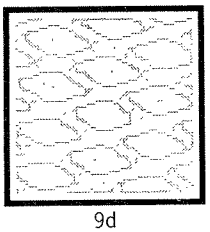

9d

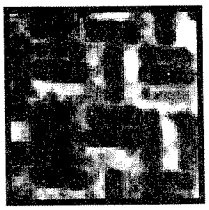

7e

(B)

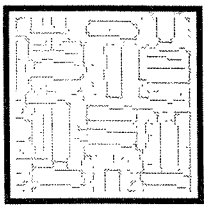

9e

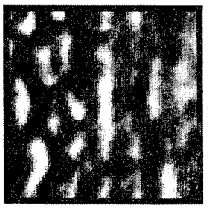

7f

(T)

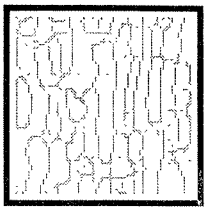

9f

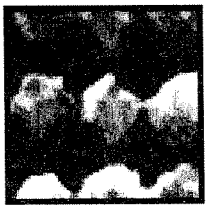

7g

(O)

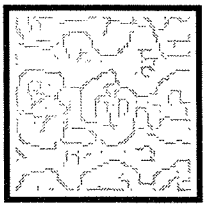

9g

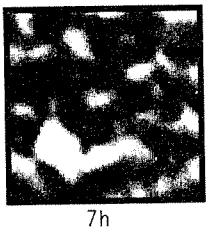

7h

(P)

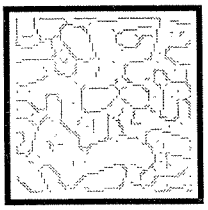

9h

Fig. 7. One normalized 64×64 sample for each class in Fig. 6. (Note: Brick samples were overlapping)

Fig. 9. Edge-pixels for samples in Fig. 7.

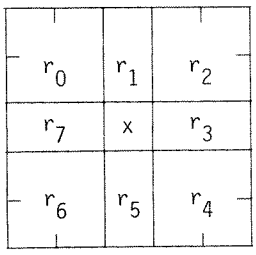

Fig. 8. Neighborhoods for the 5×5 Kirsch operator.

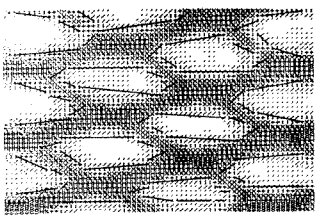

Fig. 10. Example of extended-edges.

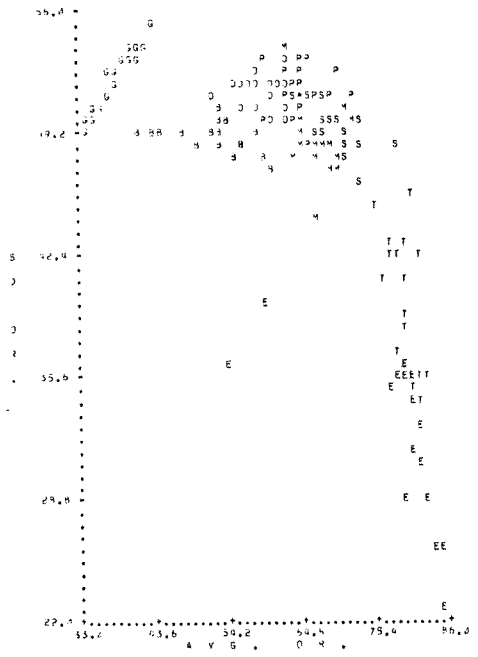

Fig. 11. Scatter plot for first-order pixel-edge statistics.

Prototype	Attribute	Spatial Predicate	Best Pair	Accuracy
pixel-intensity	intensity	S_{D_1}	contrast correlation	53%
		S_{D_2}	contrast correlation	52%
edge-pixel	orientation	S_2	correlation uniformity	55%
		S_4	contrast entropy	55%
		S_{a_3}	contrast uniformity	59%
		S_{a_7}	contrast uniformity	49%
		S_{D_3}	contrast uniformity	49%
		S_{D_7}	contrast entropy	61%
extended-edge	length/orientation	S_{a_3}	contrast correlation	36%
		S_{a_5}	contrast uniformity	49%
		S_{a_7}	contrast uniformity	52%
		S_{N_5}	contrast uniformity	32%

Table 1. Comparative results for various GCM's.

Prototype	Best Pair	Accuracy
edge-pixel	average orientation standard deviation orientation	77%
extended-edge	average orientation standard deviation orientation	64%

Table 2. First-order statistics results.